Fish Physiol Biochem (2017) 43:1387–1398
DOI 10.1007/s10695-017-0379-7

Comparative transcriptome analysis of molecular mechanism underlying gray-to-red body color formation in red crucian carp (*Carassius auratus*, red var.)

Yongqin Zhang · Jinhui Liu · Liangyue Peng · Li Ren · Huiqin Zhang · Lijun Zou · Wenbin Liu · Yamei Xiao

Received: 24 January 2017 / Accepted: 24 April 2017 / Published online: 5 July 2017

Abstract Red crucian carp (*Carassius auratus* red var.) is an ornamental fish with vivid red/orange color. It has been found that the adult body color of this strain forms a gray-to-red change. In this study, skin transcriptomes of red crucian carp are first obtained for three different stages of body color development, named by gray-color (GC), color-variation (CV), and red-color (RC) stages, respectively. From the skins of GC, CV, and RC, 103,229; 108,208; and 120,184 transcripts have been identified, respectively. Bioinformatics analysis reveals that 2483, 2967, and 4473 unigenes are differentially expressed between CV and GC, RC and CV, and RC and GC, respectively. A part of the differentially expressed genes (DEGs) are involved in the signaling pathway of pigment synthesis, such as the melanogenesis genes (*Mitfa, Pax3a, Foxd3*, *Mc1r*, *Asip*); tyrosine metabolism genes (*Tyr*, *Dct*, *Tyrp1*, *Silva*, *Tat*, *Hpda*); and pteridine metabolism genes (*Gch*, *Xdh*, *Ptps*, *Tc)*. According to the data of transcriptome and quantitative PCR, the expression of *Mitfa* and its regulated genes which include the genes of *Tyr*, *Tyrp1*, *Dct*, *Tfe3a*, and *Baxα*, decreases with gray-to-red change. It is suggested that *Mitfa* and some genes, being related to melanin synthesis or melanophore development, are closely related to the gray-to-red body color transformation in the red crucian carp. Furthermore, the DEGs of cell apoptosis and autophagy pathway, such as *Tfe3a*, *Baxα*, *Hsp70*, *Beclin1*, *Lc3*, *Atg9a*, and *Atg4a*, might be involved in the melanocytes fade away of juvenile fish. These results shed light on the regulation mechanism of gray-to-red body color transformation in red crucian carp, and are helpful to the selective breeding of ornamental fish strains.

Keywords Body color · Pigment cells · Melanogenesis · Transcriptome · Red crucian carp

Introduction

Red crucian carp (*Carassius auratus* red var.), a common goldfish, is a freshwater fish in the family Cyprinidae of order Cypriniformes. It is one of the earliest domesticated fish and became a popular ornamental fish due to its beautiful red/orange body color (Komiyama et al. 2009; Wang et al. 2013). It was found that melanocytes still occur in its embryos and juvenile skins of this strain, and then fade away with the skin color change from gray to red/orange (Liu et al. 2016). However, it remains unclear why and how the skin color changes with embryonic pigment being replaced by adult pigment in red crucian carp.

Electronic supplementary material The online version of this article (doi:10.1007/s10695-017-0379-7) contains supplementary material, which is available to authorized users.

Y. Zhang · J. Liu · L. Peng · L. Ren · H. Zhang · L. Zou · W. Liu (✉) · Y. Xiao (✉)
State Key Laboratory of Developmental Biology of Freshwater Fish, Hunan Normal University, Changsha, Hunan 410081, China
e-mail: liuweabin@163.com
e-mail: yameix@hunnu.edu.cn

Y. Zhang · J. Liu · L. Peng · L. Ren · H. Zhang · L. Zou · W. Liu · Y. Xiao
School of Life Sciences, Hunan Normal University, Changsha, Hunan 410081, China

Skin coloration is determined by some specific cells, called "pigment cells," being classified by pigment. In fish, the body color is controlled by a number of basic pigment cells, such as melanocytes, xanthophores, erythrophores, and iridocytes (Matsumoto 1965, Matsumoto and Obika 1968; Kelsh 2004). Melanocytes, containing a large number of melanin granules, are able to absorb specific wavelength of the incident light and make the fish color appear black/gray. Both xanthophores and erythrophores contain pteridine and carotenoids, which are related with yellow, orange, and red colors of the fish. Iridocytes, also known as the guanophore and white pigment cells, contain white, blue, and purple-red color crystal owing to the main material and water knot synthesis crystal forms of guanine (Fujii 2000; Oshima 2001). Differentiation and development of the pigment cells are strictly regulated under genetic control (Parichy 2006; Dooley et al. 2013). In 1994, the tyrosinase gene was first cloned from medaka *Oryzias latipes* (Inagaki et al. 1994). Up to now, about 38 and 94 genes have been found in medaka *O. latipes* and zebrafish, respectively, which are related with the body color formation (Jiang et al. 2014). Additionally, it has been found that some signaling pathways, including Wnt/β-catenin, EDN3/EDNRB, and KIT/KITL, affect the survival, proliferation, migration, and differentiation of pigment cells (Yamanaka and Kondo 2014; Mahalwar et al, 2014).

An interesting issue is to address what is the molecular mechanism of gray-to-red change in the body color development of red crucian carp. In this study, by Illumina sequencing technology, we intend to conduct transcriptomic analysis to understand the genetic profiles of red crucian carp skin tissue. Particularly, we attempt to identify the candidate genes, which are responsible for skin color differentiation from gray to red/orange. It can not only reveal the molecular mechanism in body color formation of red crucian carp but also provide useful gene information for the breeding of ornamental fish strains in aquaculture.

Materials and methods

Materials

Embryos and larvae of red crucian carp, used for this study, were collected from the State Key Laboratory of Developmental Biology of Freshwater Fish in Hunan Normal University, China. The embryos were raised in the laboratory at 23–24 °C, and the larvae were cultured in separate cement pool. All the sampling procedures were conducted according to the standards and ethical guidelines established by the Animal Ethical Review Committee of Hunan Normal University, Changsha, China.

Histological observation on pigment cells in embryos and larvae

Pieces of fresh skin were surgically excised from the larvae. For the subsequent light microscopy, the skin pieces were directly soaked in an embedding solution of optimum cutting temperature compound (Sakura Finetek, USA). Sections of 10 μm in thickness were obtained in a Leica CM3050S Frozen Microtome. Then, they were transferred to slides and directly observed without being stained. On the other hand, for electron microscopy, the small pieces of skin were fixed at 4 °C in 5% glutaraldehyde solution for 2 h, then, treated by 2% OsO_4 for 2 h. After dehydration through an ethanol series, the specimens were embedded in Epon812 resin (TAAB, USA). Ultrathin slices of specimens about 60 nm were made by ultramicrotome (Germany, Leica EM UC7). Then, the sections were doubly stained with uranyl acetate and lead citrate, and were examined by electron microscope (Japan, JEM-1230).

Construction of cDNA library and sequencing

Fresh skin tissues of fish were collected from the gray-color (GC) stage (45-day post-hatching (dph)), color-variation (CV) stage (65 dph), and red-color (RC) stage (85 dph), respectively. Each sample of skin tissue was collected from siblings, a mixture of more than six fishes. All the samples were stored in RNAlater (Ambion Life technologies, Grand Island, NY, USA) at −80 °C. Total RNA was purified using RNA TRIzol (Invitrogen, Carlsbad, CA, USA) and quantified with Agilent 2100 Bioanalyzer (Agilent, Santa Clara, CA, USA). The complementary DNA (cDNA) libraries were synthesized using the mixed messenger RNA (mRNA) fragments as templates with the TruSeq RNA sample preparation kit V2 (Illumina, San Diego, CA, USA) according to the manufacturer's instructions. The libraries were

sequenced using Illumina HiSeq 2000, at BGI Shenzhen, Guangdong, China.

De novo assembly and sequence annotation

The de novo assembly was carried out with Trinity using default parameters such that unigenes were generated. TGICL was used to reduce redundancy and further correct the assembly. Then, the sequences were processed by homologous transcript clustering to get the unigenes. Blastx alignment (E value <0.00001) between unigenes and protein databases was employed to annotate the genes.

Analysis of differentially expressed transcripts

The fragments per kilobase per million fragments mapped (FPKM) method was used to calculate the transcript expression levels. The adjusted P values were used for the false discovery rate (FDR) in multiple hypothesis testing, which deploys the Benjamini-Hochberg correction to determine the difference significance between samples. The unigenes with FDR ≤0.001 and $|\log_2 \text{Ratio}| \geq 2$ were considered as the differential expression genes for further analysis. GO enrichment analysis was carried out with the Blast2GO v2.5.0 software (Conesa et al. 2005). The GO terms with FDR <0.05 were considered to be significantly enriched.

Quantitative real-time PCR analysis

The total RNAs were extracted from the fresh skin tissues of fish at the GC, CV, and RC stages, respectively. Each RNA sample was treated by PrimeScript™ RT Reagent Kit with gDNA Eraser (Takara) to remove residual genomic DNA and reverse transcribe into cDNA. The quantitative real-time PCR (qRT-PCR) analysis was conducted using the Prism 7500 Sequence Detection 140 System (Applied Biosystems) with a miScript SYBR Green PCR kit (QIAGEN). The primers for qRT-PCR were shown in Table S1 in Supplementary, which were designed by the Primer Express® Software Primer 5.0. The PCR was carried out on the Stratagene Mx3000P instrument (Agilent, USA). For each sample, qRT-PCR analysis was done by three biological replicates.

Results and discussion

Histological observation on body color temporal change in red crucian carp

Chromatophores are mainly responsible for generation of skin color and can be further subdivided on the basis of color differences. In red crucian carp, melanocytes appeared in the embryo skin and larvae and remained dark-gray, named gray-color (GC) stage (Fig. 1a). The pigment cells, melanophores, xanthophores, and erythrophores, were all observed in the GC skin (Fig. 1d, g–i). After 2 months or so, the gray body color began fading away since the number of melanocytes is significantly decreasing in skin, which resulted in the emergence of red/orange body color (Fig. 1b, e). In this color-change stage (CV stage), its cellular structure also changes, such as the reduction of melanosomes and emergence of many vacuoles in the cytoplasm (Fig. 1j–l), as well as the number reduction of melanocytes in skins. Then, after 3 months, the gray body color of this fish completely transformed into red/orange one due to loss of melanin, the same body color as adult (Fig. 1c, f). We call this process the red-color (RC) stage.

DNA sequence generation and transcriptome assembly

Three cDNA libraries were built from the skins of fish for the three developmental stages of body color, GC, CV and RC, respectively. In Table 1, we present the Q20 percentage, N percentage, GC percentage, unigenes, and the other indexes to describe the libraries. Complete clean reads of the three libraries have been uploaded to the SRA site (http://www.ncbi.nlm.nih.). After filtering, about 52, 53, and 54 million clean reads were obtained in the skins of the GC, CV, and RC stages, respectively. The Q20 percentages obtained from the skins of GC, CV, and RC libraries were 98.07, 97.93, and 97.95%, respectively. The GC percentages were 47.22, 46.93, and 47.10%, respectively. After clustering in the TGICL software, 103,229 unigenes, with mean sizes of 542 bps and N50s of 835 bps, were assembled for the GC stage. As for the CV, 108,208 unigenes were assembled, with mean sizes of 569 bps and N50s of 945 bps. With regard to the RC, there were 120,184 unigenes to be assembled with mean sizes of 597 bps and N50s of 1038 bps.

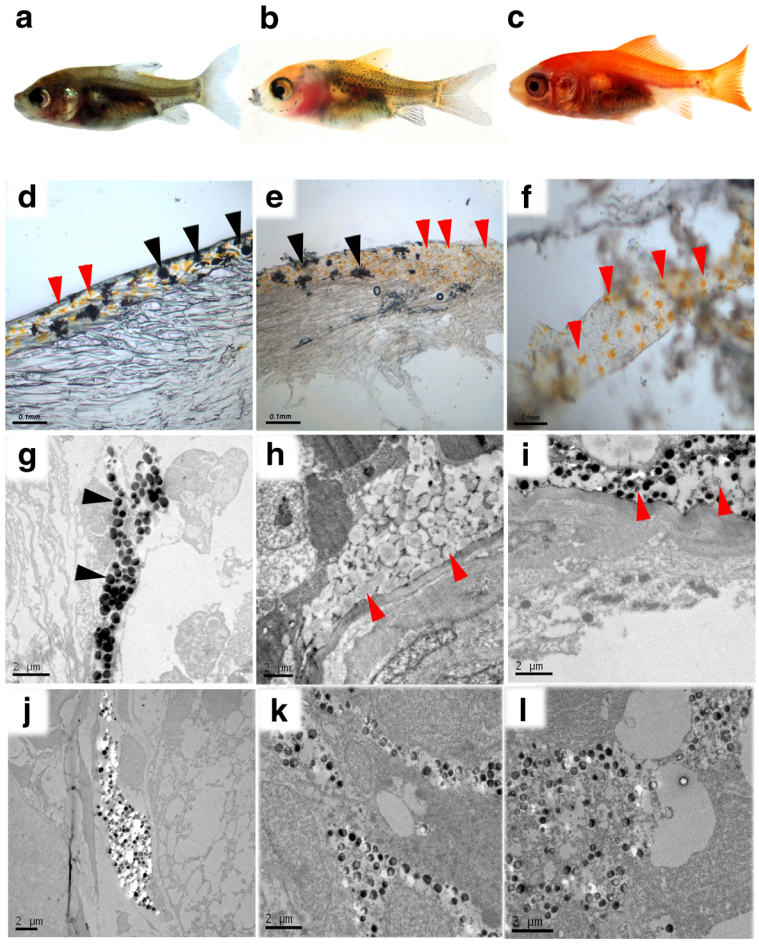

Fig. 1 Histological observation on body color temporal change in red crucian carp. **a–c** The larvae at the gray-color (GC) stage (**a**), color-variation (CV) stage (**b**), and red-color (RC) stage (**c**). **d-f** Histological observation on pigment cells in skin tissues by frozen-section. The pigment cells, which contain melanophores (*black arrow*), xanthophores, and erythrophores (*red arrow*), were observed in the GC skin (**d**) and CV skin (**e**). But there was no melanocyte in the RC skin (**f**). **g–i** The ultra-structures of melanophore (**g**), xanthophore (**h**), and erythrophore (**i**) in the GC skin. **j–l** The ultra-structures of melanophores with decrease of melanin pigment and empty vesicles in the CV skin

Functional annotation and analyses

The size distribution of unigenes is shown in Fig. 2a. There were 99,166 unigenes which could be matched to the given genes in the public databases. Analysis of identity distribution and species distribution indicates that transcriptome of red crucian carp was more closely related to that of *Danio rerio* than to the other fish genomes presented in the current public databases (Fig. 2b). Further analysis of gene ontology (GO) demonstrates that 41,940 unigenes were successfully mapped to gene ontology categories biological processes, cellular components, and molecular functions (Fig. 2c). For the biological processes, majority of the transcripts were associated with "biological regulation," "cellular process," "metabolic process," "developmental process," "multicellular organismal process," "regulation of biological process," and "single-organism process." By sequence homology, 19,414 unigenes were assigned into 25 Clusters of Orthologous Groups (COG) categories (Fig. 2d). And 47,831 unigenes were mapped to 259 predicted metabolic pathways through the KEGG database (see Table S2 in Supplementary). Main

Table 1 Overview of sequencing and assembly

Sample	GC	CV	RC
Total raw reads	55,399,804	57,546,48	58,450,968
Total clean reads	52,017,956	53,689,066	54,626,008
Total clean nucleotides	4,681,616,040	4,832,015,940	4,916,340,720
Q20 percentages	98.07%	97.93%	97.95%
N percentages	0.00%	0.01%	0.01%
GC percentages	47.22%	46.93%	47.10%
N50	835	945	1038
Mean	542	569	597
Unigenes	103,229	108,208	120,184

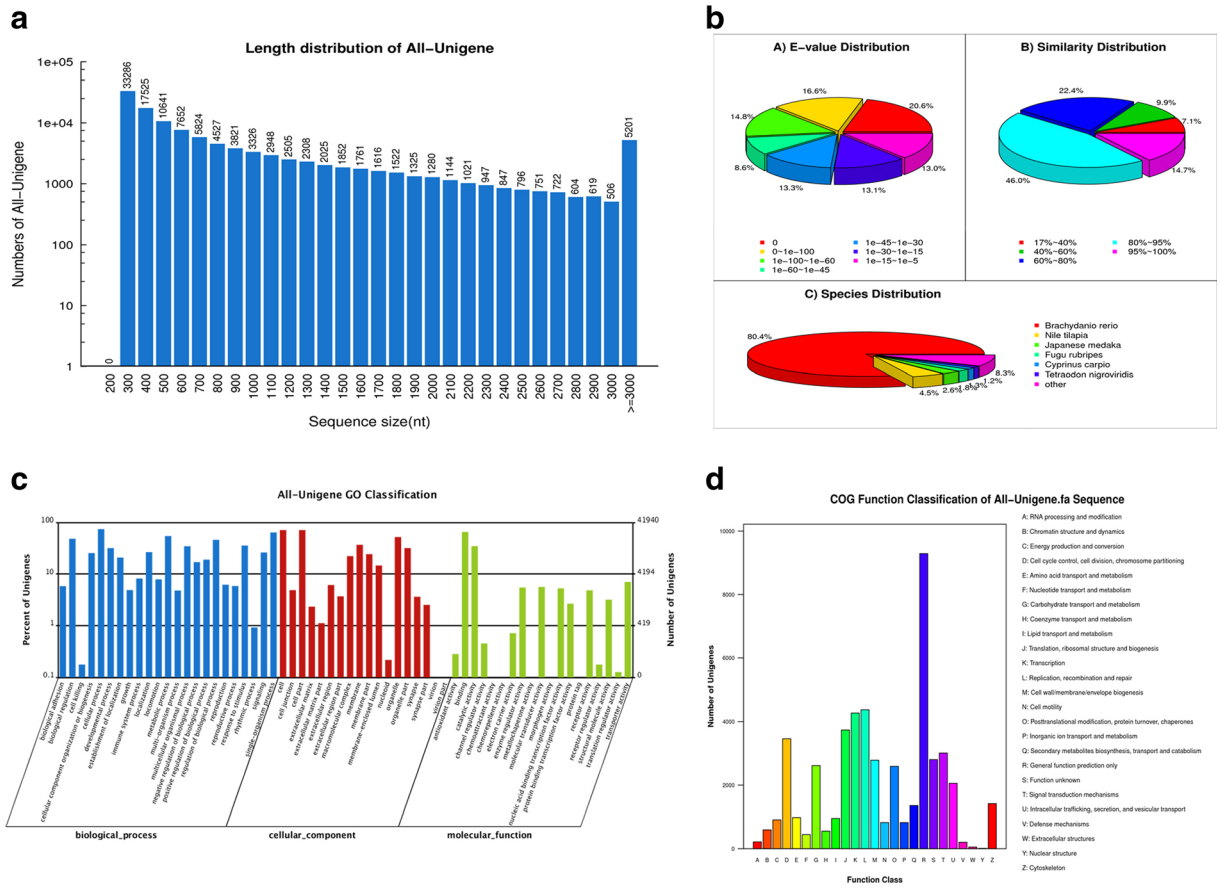

Fig. 2 Data analysis in the skin tissue transcriptome of red crucian carp. **a** Length distribution of All-unigenes. **b**: Distribution of the homology search of unigenes against the non redundant (NR) protein database. *A E* value distribution of the top Blastx hits against the NR database for each unigene; *B* Similar distribution of the top Blastx hits against the NR database for each unigene; *C* Species distribution of unigenes matching the top six species using Blastx in the NR database. **c** Histogram of GO analysis of All-Unigenes. **d** Histogram of COG classification of All-Unigenes

categories of the metabolic pathways, for instance, were the mitogen-activated protein kinase (MAPK) signaling pathway (393), p53 signaling pathway (390), cell cycle (687), tyrosine metabolism (108), melanogenesis (642), Wnt signaling pathway (197), and regulation of autophagy (72) (see Fig. S1 in Supplementary).

Comparative analysis of differentially expressed gene

Based on the criteria that FDR ≤0.001 and $|\log_2$ Ratio$|\geq 2$, it is shown that in comparison with the GC skin, 2483 unigenes were differentially expressed in the CV skin, 1604 genes out of them being upregulated and 879 genes being downregulated. With regard to the RC skin, there were 4473 unigenes to be differentially expressed, 2697 genes out of them being upregulated, and 1776 genes being downregulated in the RC skin. Compared with the CV skin, there were 2967 unigenes to be differentially expressed in the RC skin, 1923 genes out of them being upregulated and 1044 genes being downregulated (Fig. 3).

To judge the DEGs identified by transcriptomic analysis, 20 DEGs with different expression patterns in the GC and RC skins were randomly selected for further qRT-PCR assay on biological replicates. As shown in Fig. 4, out of 20 DEGs, the 18 qRT-PCR expression patterns were in agreement with the data obtained from RNA-seq, where 11 unigenes were upregulated and 7 unigenes were downregulated.

By oxidation of the amino acid tyrosine and polymerization, melanin was produced. As seen in Table 2 and Fig. 5, the mRNA expression levels of key genes for tyrosine synthesis, such as those encoding tyrosinase (TYR), tyrosinase-related protein 1 (TYRP1),

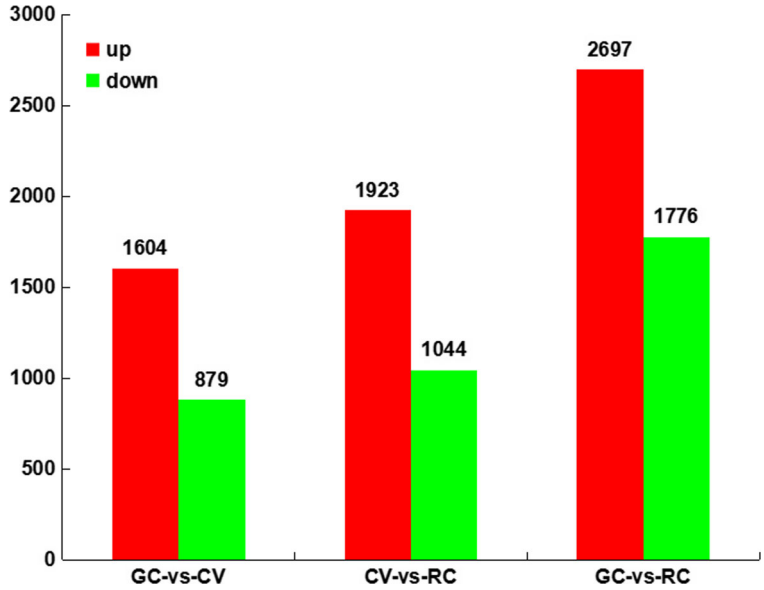

Fig. 3 Differentially expressed genes. The horizontal axis is the samples on the control of the situation, while the difference of gene number is measured by the vertical axis. There are two expression levels: upregulated expression is represented by *red color* in Fig. 3. *Green color* stands for the downregulated expression. *GC* gray-color stage skin, *CV* color-variation stage skin, *RC* red-color stage skin

dopachrome tautomerase (DCT), and silver protein (SILVa), were all downregulated in the gray-to-red stage of the red crucian carp skin. In contrast, with regard to the gray-to-red/orange stage, it follows from the data of transcriptome and the real-time PCR that the mRNA expression levels of *Mitfa* and *Pax3a* were downregulated, while that of *Foxd3* was upregulated. TYR carries out tyrosine hydroxylation to L-DOPA, which is the first step of biosynthetic pathway for melanin. Under the action of the DCT and TYRP1, the DOPA chrome was rapidly oxidized and polymerized to form dark melanin (Braasch et al. 2009; Simon et al. 2009). In zebrafish, mutation in TYRP1 causes death of melanophore that leads to a semi-dominant phenotype (Krauss et al, 2014). Among the earliest expressed genes, MITF is a master regulation factor in the melanocyte lineage (Lister et al. 1999, 2001; Steingrimsson et al. 2004; Levy et al. 2006; Zeng and Johnson 2014). It has been reported that MITF could directly regulate the expression of multiple genes being necessary for melanophore development, including *Tyr*, *Tyrp1*, and *Dct* (Tassabehji et al. 1994; Opdecamp et al. 1997; Cheli et al. 2010). It

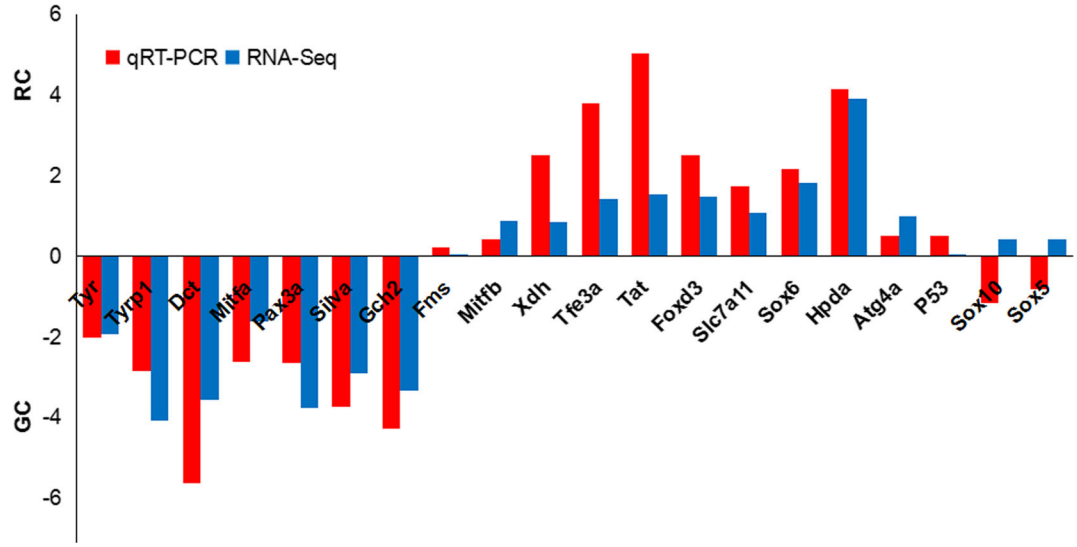

Fig. 4 Comparison of mRNA expression levels among the 20 differently expressed unigenes obtained using qRT-PCR validation and RNA sequencing. Log-fold changes are expressed as the ratio of gene expression after normalization to β-actin

Table 2 Analysis of differentially expressed genes related to development of pigment cells

Pathway	Gene	GC_FPKM	CV_FPKM	RC_FPKM	Note
Melanogenesis	Wnt2b	2.28	1.10	0.54	Wnt family member 2b
	Wnt5b	13.58	6.60	6.22	Wnt family member 5b
	Pax3a	11.6	1.95	1.79	Paired box protein Pax-3a
	Sox10	6.06	5.31	5.82	Transcription factor SOX-10
	Mitfa	3.96	1.29	0.64	Microphthalmia associated transcription factor a
	Mitfb	2.03	2.99	3.75	Microphthalmia associated transcription factor b
	Mc1r	2.36	1.75	0.86	Melanocortin receptor 1 gene
	Asip	1.81	3.42	5.44	Agouti-signaling protein
	Foxd3	4.61	10.96	8.11	Forkhead box D3
	Edn3	8.95	6.19	1.79	Endothelin-3
	Ednra	3.65	2.38	1.53	Endothelin receptor type A
Tyrosine metabolism	Tyr	4.11	2.99	1.09	Tyrosinase
	Tyrp1	7.31	6.16	0.43	Tyrosinase-related protein 1
	Dct	2.52	0.42	0.11	Dopachrome tautomerase
	Silva	5.54	6.51	0.62	Silver protein a
	Tat	13.77	40.39	43.19	Tyrosine aminotransferase
	Hpda	6.82	28.26	43.48	4-hydroxyphenylpyruvate dioxygenase a
	Hgd	33.68	17.53	14.71	Homogentisate1,2-dioxygenase
	Fah	17.22	10.04	7.13	Fumarylacetoacetate hydrolase
	Pah	12.91	24.17	15.51	Phenylalanine hydroxylase
Pteridine metabolism	Gch2	12.08	3.68	1.19	GTP cyclohydrolase 2
	Xdh	1.02	1.02	1.86	Xanthine dehydrogenase/oxidase
	Slc7a11	3.01	2.94	6.38	Solute carrier family 7, member 11
	Ltk	2.82	1.71	1.74	Leukocyte tyrosine kinase
	Slc3a2b	52.99	208.02	193.94	Solute carrier family 3, member 2b
	Sox5	2.82	2.87	3.07	Transcription factor SOX5
	Sox6	0.57	1.11	2.05	SRY-box containing gene 6
	Kita	4.64	2.41	3.89	Kit a protein
	Tc	8.32	11.63	22.95	Transcobalamin-2
	Plb	2.89	8.24	18.28	Phospholipase B1, membrane-associated
	Gch1	4.48	6.47	10.68	GTP cyclohydrolase 1
	Ptps	1.87	4.57	8.42	6-pyruvoyl tetrahydropterin synthase
Apoptosis and autophagy	Gpib	8.31	9.82	4.54	Glucose phosphate isomerase b
	Caspase3	.54	3.63	5.48	Apoptosis-related cysteine protease 3
	Bax_{α}	6.65	7.88	11.97	Bcl2-associated X protein alpha
	Beclin1	6.84	10.34	25.72	Beclin 1-associated protein
	Lc3	15.04	17.79	28.42	Microtubule-associated light chain 3
	Atg9a	3.64	6.09	8.35	Autophagy-related 9 homolog A
	Atg4a	4.06	5.24	13.88	Autophagy-related 4 homolog A
	Tfe3a	3.64	5.67	9.08	Transcription factor binding to IGHM enhancer 3a
	P53	4.88	4.12	4.75	Tumor suppressor protein p53
	C-fos	136.86	105.47	7.48	C-Fos protein
	Hsp70	10.29	27.25	44.34	Hsp70 protien
	Ttr	0.84	14.37	13.98	Transthyretin

Table 2 (continued)

Pathway	Gene	GC_FPKM	CV_FPKM	RC_FPKM	Note
	Tshr	2.34	3.24	6.45	Thyroid stimulating hormone receptor
	Hiomt	1.97	2.52	3.44	Hydroxindole-O-methyltransferase
	Adcy2b	6.58	7.21	10.39	Adenylate cyclase 2b
	Mapk8ip3	5.97	6.67	10.72	C-Jun-amino-terminal kinase-interacting protein 3

is well known that the paired box protein Pax-3a (*Pax3a*) is an MITF-inducible pigment cell-specific gene, the mutations in the *Pax3* cause Waardenburg syndrome (WS) with extensive overlap in melanophores defect as seen with MITF mutations (Bejar et al. 2003). It was reported that the expression of mitfa could be regulated by *Foxd3*, where the former was positive regulation, while the latter for the negative control (Steingrimsson et al. 2004; Lacosta et al. 2005; Curran et al. 2009; Thomas and Erickson 2009). Our results further confirm that the tyrosine metabolism pathways regulated by *Mitfa* are involved in the downregulation of melanogenesis, which causes the gray-to-red/orange color transformation in red crucian carp.

It is clear that the differentially expressed genes shown in Fig. 5 were related to the pigment cell development in the skins at the different color stages in red crucian carp. Furthermore, from our transcriptome data, it follows that the mRNA expression level of *Tat*, *Hpda*, and *Tfe3a* were upregulated in the skin from the GC to the RC stage (Table 2 and Fig. 5). In the tyrosine metabolic pathways, tyrosine can generate homogentisic acid under the catalysis reaction of tyrosine aminotransferase (TAT) and 4-hydroxyphenylpyruvate dioxygenase (HPDA). The homogentisate1, 2-dioxygenase catalysis homogentisic acid generates melatonin. The higher-level *Tat* and *Hpda* would directly reduce tyrosine level, thereby inhibiting the synthesis of melanin (Zhang et al. 2008). Nonetheless, the transcription factor binding to IGHM enhancer 3a (*Tfe3a*), one homologous gene of *Mitf*, is capable of activating transcription through *Mitf* binding sites. In mammal, *Tfe3a* can activate reporters driven by the native tyrosinase promoters in cell culture as well as or better than *Mitf* (Weilbaecher et al. 1998). But although relative to the *Mitf*, *Tfe3a* could not activate the transcription of *Dct*, which is an important key of the melanin synthesis enzyme. Therefore, *Tfe3a* was inefficiently supported melanocyte development when expressed in neural crest cells of embryos lacking *Mitf* (Steingrímsson et al. 2002). Our results suggest that *Tfe3a* might be controlled by negative regulation or competitive inhibition of the expression of *Mitfa*, which controlled the melanin synthesis along with its enzymatic regulation by the *Tyr* gene family during the body color transformation of red crucian carp.

Comparing the GC, CV, and RC skin transcriptome, it is noted that some genes were involved in the biosynthetic pathway for erythrosome and xanthosome. The mRNA expression level of *Xdh*, *Gch1*, and *Ptps* was significantly upregulated in the RC skin in comparison with the GC skin (Table 2), which directly contributes to the increment of erythrophores and xanthophores after the CV stage in red crucian carp. It was well established that erythrophores and xanthophores contain two kinds of pigments: pteridines and carotenoids (Masada et al. 1990). As with other vertebrates, teleost is unable to synthesize carotenoids de novo and relies solely on dietary supply to achieve their related red/orange to yellow skin pigmentation (Nickell and Springate 2001). The pteridine pathway has substrate guanosine triphosphate (GTP), which is converted by GTP cyclohydrolase I (GCH1) followed by 6-pyruvoyl tetrahydropterin synthase (PTPS) into 6-pyruvoyl tetrahydropterin. Actually, the xanthine dehydrogenase (XDH) is also involved in the pteridine pigment synthesis (Ziegler et al. 2000).

Our results demonstrate that the mRNA level of the melanocortin 1 receptor (*Mc1r*) gene was downregulated as the body color change from gray-to-red change in red crucian carp. In contrast, the mRNA levels of agouti-signaling protein (*Asip*) gene was upregulated in this process of body color change (Table 2). *Mc1r* gene is a key gene in melanogenesis in animals. The alpha-melanocyte stimulating hormone (α-MSH) binds to MC1R, resulting in reduction of cAMP level. Consequently, the melanin biosynthesis process was triggered (Voisey et al. 2001). As an endogeneous antagonist of α-MSH, ASIP could generate melanin synthesis blocked by competing with α-MSH for binding to the MC1R (Sakai et al. 1997). The xCT (SLC7A11), a

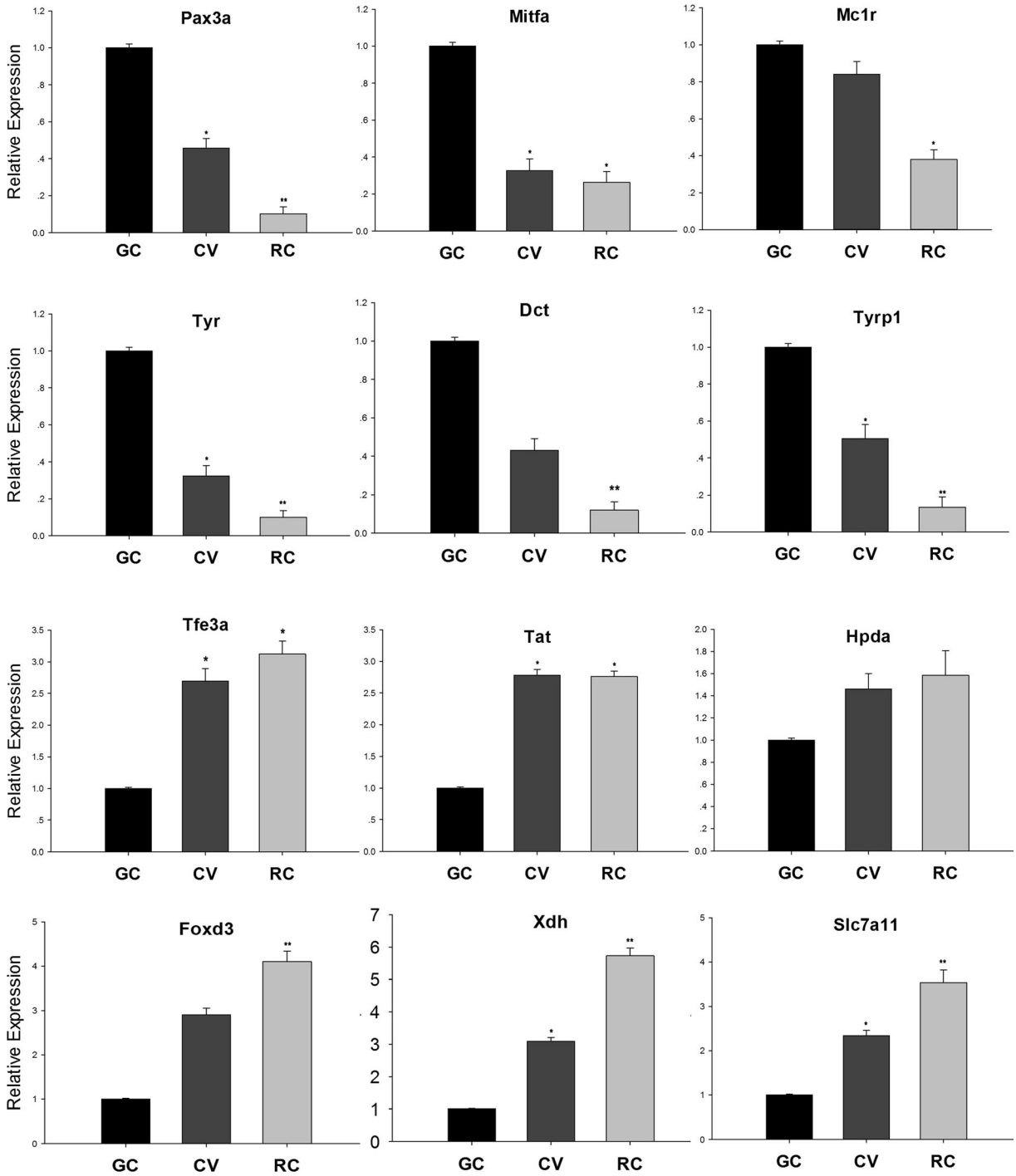

Fig. 5 Real-time PCR analysis for a part of the differentially expressed genes. The *lowercase letters* show the significant differences (*$P < 0.05$) (means ± SD of relative expression; $n = 3$ for each group)

cysteine/glutamate exchanger, mediates the cellular absorption cysteine (Lim and Donaldson 2011), which is a critical component of pheomelanin and directly affects the melanin synthesis (Chintala et al. 2005). In addition, we found that thyroid-stimulating hormone receptor (TSHR) and transthyretin (TTR), a thyroid hormone transporters protein, were all upregulated significantly in the RC skin, compared with the GC skin in red

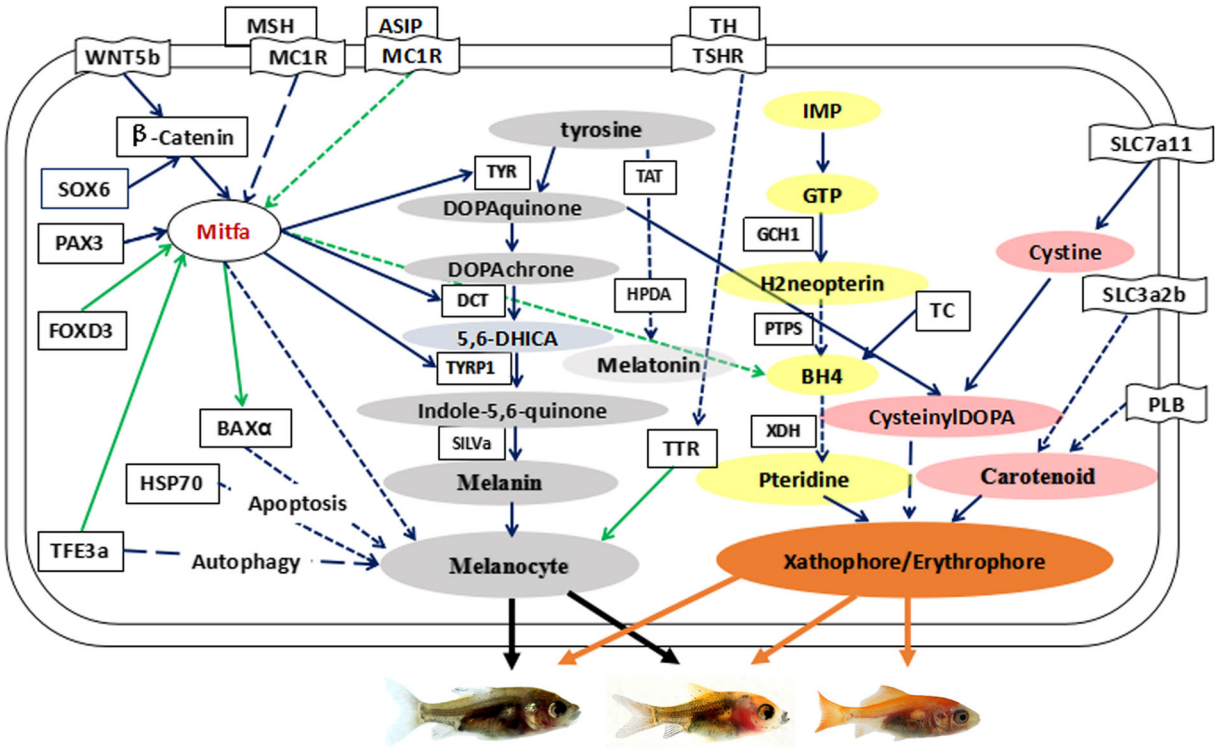

Fig. 6 Genes known be associated with pigmentation biosynthesis signaling pathways

crucian carp (Table 2). It has been reported that the thyroid hormone (TH) plays an important role in repressing homeostatic melanocyte numbers, and the mutation in TSHR can lead to a loss of melanocytes and an increase in xanthophores (Shah et al. 2006; McMenamin et al. 2014).

Enrichment and pathway analysis of differentially expressed genes

To explore whether the mechanism underlying gray-to-red body color formation of red crucian carp is controlled by multiple agents via pathways or not, we made a comparison among the GC, CV, and RC skin transcriptomes. By enrichment and pathway analysis on the differentially expressed genes, we can answer what are the key genes which affect the signaling pathway related to the color changes in red crucian carp. The top ten signaling pathways from GC to CV or from CV to RC were compared in this study. It is found that the differentially expressed genes from GC to CV include the complement and coagulation cascades (206), protein digestion and absorption (247), vitamin digestion and absorption (56), and fat digestion and absorption (67) signaling pathways. The differentially expressed genes from CV to RC contain mineral absorption (73), vitamin digestion and absorption (42), and fat digestion and absorption (45) signaling pathways (see Table S4 in Supplementary).

Listed from the skin tissues of GC, CV, and RC, a set of DEGs, with which not only belong to the pigments biosynthesis pathways, chromatophores differentiation pathways, but also to autophagy and apoptosis pathways, were assigned to control the gray-to-red body color transformation in red crucian carp (Table 2 and Fig. 6). Actually, the mRNA levels of apoptosis genes, such as Hsp70 and Baxα, increase significantly in the body color transformation from the GV skin to the CV and RC skins (Table 2). Meanwhile, the mRNA levels of Beclin1, Lc3, Atg4a, and Atg9a, as the autophagy genes, were all upregulated in the GC skin comparing to RC skin. As a member of the heat shock protein (HSP) family, HSP70 was shown to play a critical role in protein folding which can result in signal transduction, apoptosis, protein homeostasis, and cell growth and differentiation (Jun et al. 2016; Najafizadeh et al. 2015). BAX_{α}, a homologous protein with BCL-2, could determine survival or death by an apoptotic stimulus. Over-expression of BAX_{α} could

result in an accelerated rate of cell death (Oltvai et al. 1993). *Beclin1*, a mammalian ortholog of the yeast autophagy-related gene 6 (Atg6), interacts with either BCL-2 or PI3k class III, which plays a critical role in the regulation of both autophagy and cell death (Liang et al. 1998; Takacs-Vellai et al. 2005). The microtubule-associated protein light chain 3 (MAP-LC3), referred to as LC3, is involved in the formation of autophagy, and is proved to be one of the autophagy marker proteins in mammalian cells.

It has been reported that the amphibian xanthophores could be transformed into functional melanophores (Bagnara et al. 1978). In goldfish, erythrophores and xanthophores were in a labile state ready to undergo melanogenesis since L-Tyrosine was detected (Masada et al. 1990), and goldfish melanophores had a considerable capacity for pteridine biosynthesis, including the yellow pigment sepiapterin (Ben et al. 2003). However, there is no proof to confirm that the melanophores could be transformed into xanthophores or erythrophores in the process of body color change from gray to red in red crucian carp.

Conclusions

The transcriptomes of skin at the three developmental stages of body color have been obtained in red crucian carp. There were 2483, 2967, and 4473 transcripts in total, being differentially expressed between CV and GC, RC and CV, RC and GC, respectively. Comparing the GC, CV, and RC skin transcriptome, it has been shown that lower-level expression of *Mitfa* and its inactivation stimulate the transcription of Tyr, Tyrp1, and Dct, and were responsible for the downregulated synthesis of melanin that causes the gray-to-red/orange body color transformation in red crucian carp. It is suggested that body color formation in red crucian carp may be subject to complex controls by multiple agents via pathways, not only the pigments biosynthesis pathway, chromatophores differentiation pathway, but also the autophagy and apoptosis pathways. However, the interaction details of the melanogenesis with the other regulatory pathways, such as pteridine synthesis pathway, endocrine regulation system, or autophagy and apoptosis pathway, are worth being further investigated. The exploration of body color formation in red crucian carp provides insight into the genetic regulation mechanism of fish, especially some useful gene information for the breeding of improved ornamental fish strains.

Acknowledgments This work has been supported by the National Science Foundation of China (31472272), the National Basic Research Program of China (2012CB722305), Hunan Provincial Natural Science Foundation of China (14JJ2058), the Scientific Research Fund of Hunan Provincial Education Department (15C0841 and 14FJ4261), and the Cooperative Innovation Center of Engineering and New Products for Developmental Biology of Hunan Province (20134486). The authors would like to express their thanks to the anonymous referees for their constructive comments on the paper, which have greatly improved its presentation.

References

Bagnara JT, Frost SK, Matsumoto J (1978) On the development of pigment patterns in amphibians. Am Zool 18:301–312

Bejar J, Hong Y, Schartl M (2003) Mitf expression is sufficient to direct differentiation of Medaka blastula derived stem cells to melanocytes. Development 130:6545–6553

Ben J, Lim TM, Phang VPE, Chan WK (2003) Cloning and tissue expression of 6-pyruvoyl tetrahy-dropterin synthase and xanthine dehydrogenase from *Poecilia reticulata*. Mar Biotechnol 5:568–578

Braasch I, Liedtke D, Volff JN, Schartl M (2009) Pigmentary function and evolution of tyrp1 gene duplicates in fish. Pigm Cell Melanoma R 22(6):839–850

Cheli Y, Ohanna M, Ballotti R, Bertolotto C (2010) Fifteen-year quest for microphthalmia-associated transcription factor target genes. Pigm Cell Melanoma R 23:27–40

Chintala S, Li W, Lamoreux ML, Ito S, Wakamatsu K, Sviderkaya EV, Bennett DC, Park YM, Gahl WA, Huizing M, Spritz RA, Ben S, Novak EK, Tan J, Swank RT (2005) Slc7a11 gene controls production of pheomelanin pigment and proliferation of cultured cells. P Natl Acad Sci USA 102:10964–10969

Conesa A, Gotz S, Garcia-Gomez JM, Terol J, TalonM RM (2005) Blast2GO: a universal tool for annotation, visualization and analysis in functional genomics research. Bioinformatics 21:3674–3676

Curran K, Raible DW, Lister JA (2009) Foxd3 controls melanophore specification in the zebrafish neural crest by regulation of Mitf. Dev Biol 332:408–417

Dooley CM, Mongera A, Walderich B, Nü slein-Volhard C (2013) On the embryonic origin of adult melanophores: the role of ErbB and kit signalling in establishing melanophore stem cells in zebrafish. Development 140:1003–1013

Fujii R (2000) The regulation of motile activity in fish chromatophores. Pigment Cell Res 13:300–319

Inagaki H, Bessho Y, Koga K, Hori H (1994) Expression of the tyrosine-encoding gene in a colorless melanophore mutant of the medaka fish (Oryzias kztipe). Gene 150:319–324

Jiang Y, Jiang Y, Zhang S, Xu J, Feng J, Mahboob S, Al-Ghanim KA, Sun X, Xu P (2014) Comparative transcriptome analysis reveals the genetic basis of skin color variation in common carp. PLoS One 9:e108200

Kelsh RN (2004) Genetics and evolution of pigment patterns in fish. Pigment Cell Res 17:326–336

Komiyama T, Kobayashi H, Tateno Y, Inoko H, Gojobori T, Ikeo K (2009) An evolutionary origin and selection process of goldfish. Gene 430:5–11

Krauss J, Geiger-Rudolph S, Koch I, Nusslein-Volhard C, Irion U (2014) A dominant mutation in tyrp1A leads to melanophore death in zebrafish. Pigm Cell Melanoma R 27:827–830

Lacosta AM, Muniesa P, Ruberte J, Sarasa M, Dominguez L (2005) Novel expression patterns of Pax3/Pax7 in early trunk neural crest and its melanocyte and non-melanocyte lineages in amniote embryos. Pigment Cell Res 18:43–51

Levy C, Khaled M, Fisher DE (2006) MITF: master regulator of melanocyte development and melanoma oncogene. Trends Mol Med 12:406–414

Liang XH, Kleeman LK, Jiang HH, Gordon G, Goldman JE, Berry G, Herman B, Levine B (1998) Protection against fatal Sindbis virus encephalitis by beclin, a novel Bcl-2-interacting protein. J Virol 72:8586–8596

Lim JC, Donaldson PJ (2011) Focus on molecules: the cystine/glutamate exchanger (system x(c)(2)). Exp Eye Res 92:162–163

Lister JA, Robertson CP, Lepage T, Johnson SL, Raible DW (1999) Nacre encodes a zebrafish microphthalmia-related protein that regulates neural-crest-derived pigment cell fate. Development 126:57–67

Lister JA, Close J, Raible DW (2001) Duplicate mitf genes in zebrafish: complementary expression and conservation of melanogenic potential. Dev Biol 237:333–344

Liu JH, Zhang YQ, Gui SY, Liu WB, Xiao J, Xiao YM (2016) Observation and regression models on body colour inheritance and development in crucian carp and carp. Aquacult Int 24:1191–1199

Mahalwar P, Walderich B, Singh AP, Nüsslein-Volhard C (2014) Local reorganization of xanthophores fine-tunes and colors the striped pattern of zebrafish. Science 345:1362–1364

Masada M, Matsumoto J, Akino M (1990) Biosynthetic pathways of pteridines and their association with phenotypic expression in vitro in normal and neoplastic pigment cells from goldfish. Pigment Cell Res 3:61–70

Matsumoto J (1965) Studies on fine structure and cytochemical properties of erythrophores in swordtail,Xiphophorus Helleri, with special reference to their pigment granules (pterinosomes). J Cell Biol 27:493–504

Matsumoto J, Obika M (1968) Morphological and biochemical characterization of goldfish erythrophores and their pterinosomes. J Cell Biol 39:233–250

McMenamin SK, Bain EJ, McCann AE, Patterson LB, Eom DS (2014) Thyroid hormone-dependent adult pigment cell lineage and pattern in zebrafish. Science 345:1358–1361

Nickell DC, Springate JRC (2001) Pigmentation of farmed salmonids. In: Kestin SC, Warris PD (eds) Fish farmed quality. Blackwell Science, Oxford, pp 58–75

Oltvai ZN, Milliman CL, Korsmeyer SJ (1993) Bcl-2 heterodemerizes conserved homolog Bax accelerates programmed cell death. Cell 74:609–619

Opdecamp K, Nakayama A, Nguyen MT, Hodgkinson CA, Pavan WJ, Arnheiter H (1997) Melanocyte development in vivo and in neural crest cell cultures: crucial dependence on the Mitf basic-helix-loop-helix-zipper transcription factor. Development 124:77–86

Oshima N (2001) Direct reception of light by chromatophores of lower vertebrates. Pigment Cell Res 14:312–319

Parichy DM (2006) Evolution of danio pigment pattern development. Heredity 97:200–210

Sakai C, Ollmann M, Kobayashi T, Abdel-Malek Z, Muller J, Vieira WD, Imokawa G, Barsh GS, Hearing VJ (1997) Modulation of murine melanocyte function in vitro by Agouti signal protein. EMBO J 16:3544–3552

Shah M, Orengo IF, Rosen T (2006) High prevalence of hypothyroidism in male patients with cutaneous melanoma. Dermatol Online J 12(2). John D Simon

Simon DJ, Peles D, Wakamatsu K, Ito S (2009) Current challenges in understanding melanogenesis: bridging chemistry, biological control, morphology and function. Pigm Cell Melanoma R 22:563–579

Steingrímsson E, Tessarollo L, Pathak B, Hou L, Arnheiter H, Copeland NG, Jenkins NA (2002) Mitf and Tfe3, two members of the Mitf-Tfe family of bHLH-zip transcription factors, have important but functionally redundant roles in osteoclast development. Proc Natl Acad Sci U S A 99:4477–4482

Steingrimsson E, Copeland NG, Jenkins NA (2004) Melanocytes and the microphthalmia transcription factor network. Annu Rev Genet 38:365–411

Takacs-Vellai K, Vellai T, Puoti A, Passannante M, Wicky C, Streit A, Kovacs AL, Müller F (2005) Inactivation of the autophagy gene bec-1 triggers apoptotic cell death in *C. elegans*. Curr Biol 15(16):1513–1517

Tassabehji M, Newton VE, Read AP (1994) Waardenburg syndrome type 2 caused by mutations in the human microphthalmia (MITF) gene. Nat Genet 8:251–255

Thomas AJ, Erickson CA (2009) FOXD3 regulates the lineage switch between neural crest-derived glial cells and pigment cells by repressing MITF through a non-canonical mechanism. Development 136:1849–1858

Voisey J, Box NF, van Daal A (2001) A polymorphism study of the human agouti gene and its association with MC1R. Pigment Cell Res 14:264–267

Wang SY, Luo J, Murphy RW, Wu SY, Zhu CL, Gao Y, Zhang Y (2013) Origin of Chinese goldfish and sequential loss of genetic diversity accompanies new breeds. PLoS One 8:e59571

Weilbaecher KN, Hershey CL, Takemoto CM, Horstmann M, Hemesath TJ, Tashjian AH, Fisher DE (1998) Age-resolving osteopetrosis: a rat model implicating microphthalmia and the related transcription factor TFE3. J Exp Med 187:775–785

Yamanaka H, Kondo S (2014) In vitro analysis suggests that difference in cell movement during direct interaction can generate various pigment patterns in vivo. Proc Natl Acad Sci U S A 111:1867–1872

Zeng Z, Johnson S, Lister JA, Patton EE (2014) Temperature-sensitive splicing of mitfa by an intron mutation in zebrafish. Pigm cell Melanoma R 28(2):229–232

Zhang Y, Wang L, Zhang S, Yang H, Tan H (2008) hmgA, transcriptionally activated by HpdA, influences the biosynthesis of actinorhodin in Streptomyces Coelicolor. FEMS Microbiol Lett 280(2):219–225

Ziegler I, McDonald T, Hesslinger C, Pelletier I, Boyle P (2000) Development of the pteridine pathway in the zebrafish, *Danio rerio*. J Biol Chem 275:18926–18932